



Effects of the adenosine A_{2A} receptor antagonist KW6002 on the dopaminergic system, motor performance, and neuroinflammation in a rat model of Parkinson's disease

Kavya Prasad ^a, Erik F.J. de Vries ^{a,*}, Esther van der Meiden ^a, Rodrigo Moraga-Amaro ^a, Daniel Aaron Vazquez-Matias ^a, Lara Barazzuol ^b, Rudi A.J.O. Dierckx ^a, Aren van Waarde ^a

^a Department of Nuclear Medicine and Molecular Imaging, University of Groningen, University Medical Center Groningen, Hanzeplein 1, 9713 GZ, Groningen, the Netherlands

^b Department of Biomedical Sciences of Cells and Systems, University of Groningen, University Medical Center Groningen, Hanzeplein 1, 9713 GZ, Groningen, the Netherlands

ARTICLE INFO

Handling editor: T. Di Paolo

Keywords:

A_{2A} receptor
D₂ receptor
Animal model
Parkinson's disease
Positron emission tomography
A_{2A} receptor antagonist

ABSTRACT

Adenosine A_{2A}-receptors (A_{2A}R) and dopamine D₂-receptors (D₂R) are known to work together in a synergistic manner. Inhibiting A_{2A}R by genetic or pharmacological means can relieve symptoms and have neuroprotective effects in certain conditions. We applied PET imaging to evaluate the impact of the A_{2A}R antagonist KW6002 on D₂R availability and neuroinflammation in an animal model of Parkinson's disease. Male Wistar rats with 6-hydroxydopamine-induced damage to the right striatum were given 3 mg/kg of KW6002 daily for 20 days. Motor function was assessed using the rotarod and cylinder tests, and neuroinflammation and dopamine receptor availability were measured using PET scans with the tracers [¹¹C]PBR28 and [¹¹C]raclopride, respectively. On day 7 and 22 following 6-OHDA injection, rats were sacrificed for postmortem analysis. PET scans revealed a peak in neuroinflammation on day 7. Chronic treatment with KW6002 significantly reduced [¹¹C]PBR28 uptake in the ipsilateral striatum [normalized to contralateral striatum] and [¹¹C]raclopride binding in both striata when compared to the vehicle group. These imaging findings were accompanied by an improvement in motor function. Postmortem analysis showed an 84% decrease in the number of Iba-1⁺ cells in the ipsilateral striatum [normalized to contralateral striatum] of KW6002-treated rats compared to vehicle rats on day 22 ($p = 0.007$), corroborating the PET findings. Analysis of tyrosine hydroxylase levels showed less dopaminergic neuron loss in the ipsilateral striatum of KW6002-treated rats compared to controls on day 7. These findings suggest that KW6002 reduces inflammation and dopaminergic neuron loss, leading to less motor symptoms in this animal model of Parkinson's disease.

1. Introduction

Parkinson's disease (PD) is the second most common neurodegenerative disease. The prevalence of PD increases with age, and it is estimated that about 4% of people over the age of 80 have the disease (Ray Dorsey et al., 2016). The disease pathology is characterized by degeneration of dopaminergic neurons in the *substantia nigra pars compacta* (SNc) (Kalia and Lang, 2015; Tysnes and Storstein, 2017). This progressive degeneration leads to a decrease in dopamine release with a subsequent reduction in dopamine input to the striatum, the principal recipient of dopaminergic innervation by the SNc (Calabresi et al., 2013;

Galvan et al., 2015). The striatum consists mainly of GABAergic spiny projection neurons that either play a role in the direct or indirect pathway of the basal ganglia (Gerfen and Surmeier, 2011; Zhai et al., 2019). In a healthy brain, firing of direct pathway striatal neurons causes disinhibition to the thalamic neurons, allowing them to excite the cortical neurons. The net result of exciting the direct pathway is the initiation and execution of movements. On the other hand, the firing of the indirect pathway striatal neurons makes inhibitory connections to the thalamus and suppresses movements (Galvan et al., 2015). A balanced regulation of the direct and indirect pathways of basal ganglia results in smooth movements. However, loss of dopaminergic neurons in

* Corresponding author.

E-mail address: e.f.j.de.vries@umcg.nl (E.F.J. de Vries).

PD will result in a decreased activity of the direct pathway and an increased activity of the indirect pathway, resulting in motor deficits such as tremor, rigidity and bradykinesia (Tysnes and Storstein, 2017).

Dopamine D₂ receptors (D₂R) are G protein-coupled receptors that are highly expressed in the GABAergic striatopallidal neurons of the basal ganglia (Ferré et al., 2018). In these neurons, the D₂R co-localizes with the adenosine A_{2A} receptor (A_{2A}R) to form heteromer complexes. The receptors within A_{2A}/D₂R heteromeric complexes have allosteric interactions, in which an A_{2A}R agonist induces an antagonistic effect on the D₂R (Ferré et al., 2018). Activation of the A_{2A}R leads to reduced affinity and response of D₂R for their own ligands (Agnati et al., 2003; Fuxe et al., 2003; Hillion et al., 2002). This decrease in D₂R signaling increases the activity of the GABAergic spiny projection neurons of the striatum, thereby enhancing the output of the indirect pathway (Galvan et al., 2015). Adenosine A_{2A} receptors (A_{2A}R) are predominantly located in synapses and are known to regulate various cellular functions. While these receptors have physiological roles, their overactivation has been linked to detrimental outcomes, particularly in the context of neurodegenerative diseases like Parkinson's. The cellular mechanisms underlying A_{2A}R-mediated neurodegeneration remain poorly characterized, but evidence suggests that A_{2A}R activation can enhance glutamate release, increase calcium entry, and augment long-term potentiation, all of which are actions expected to promote excitotoxic damage. Additionally, the role of adenosine production and release is a critical factor in this context, as it is the increased availability of adenosine that binds to and activates A_{2A}R, thereby influencing neuronal excitability and contributing to the pathophysiology of neurodegeneration (Cunha, 2016). Currently, the first line of treatment for PD consists of the dopamine agonist levodopa (L-DOPA) that can diminish the movement deficits and therefore decrease the clinical symptoms (Fahn, 2008). However, side effects, such as fluctuating motor performance and dyskinesias, occur frequently in prolonged L-DOPA treated patients (Vaa-monde et al., 2003). In PD patients who suffer from these effects, A_{2A}R activation with an agonist results in the inhibition of the motor cortex and the suppression of the initiation and execution of movements (Morelli et al., 2009). In contrast, treatment with A_{2A}R antagonists may enhance the D₂R mediated locomotor activity (Morelli et al., 2009). Administration of an A_{2A}R antagonist could therefore be a potential alternative therapeutic strategy to enhance the D₂R signaling, which may induce less side-effects than L-DOPA (Morelli et al., 2009; Obeso et al., 2008; Ikeda et al., 2002). A_{2A} antagonists may restore the balance between the direct and indirect pathways and may reduce the characteristic motor deficits (Richardson et al., 1997). In a landmark decision reached in 2019, the U.S. Food and Drug Administration (FDA) granted approval for Nourianz® (KW6002) as an adjunctive treatment to levodopa in Parkinson's disease (PD) patients experiencing "OFF" episodes. KW6002 operates as an adenosine A_{2A} receptor antagonist, thereby introducing a novel mechanism of action in the therapeutic landscape of PD. This seminal FDA approval not only expands the treatment options for PD but also paves the way for further exploration into the utility of adenosine A_{2A} receptor antagonists in addressing mood and cognitive deficits in PD as well as other neuropsychiatric disorders (Chen and Cunha, 2020). Our study investigates the effects of KW6002 not as an adjunctive therapy but as a standalone treatment, which could offer additional insights into its therapeutic potential.

A prominent feature of PD is an enhanced inflammatory response impelled by microglial cells (Tufekci et al., 2012). Microglia execute many functions that are thought to play a role in brain connectivity and network development (Aguzzi et al., 2013; Li and Barres, 2018). Moreover, microglia contribute to maintaining brain homeostasis by continuously scanning for plaques, damaged neurons and pathogens and acting as macrophages (Li and Barres, 2018; Gehrmann et al., 1995). On the one hand, activated microglia boost the inflammatory response and induce the release of neuronal survival factors to stimulate the repair of damaged tissue (Ramesh et al., 2013). On the other hand, microglia can produce reactive oxygen species and pro-inflammatory cytokines that

are neurotoxic (Ramesh et al., 2013; Bennett and Viaene, 2021). In chronic inflammation, persistent microglial activation enhances the inflammatory response (Bennett and Viaene, 2021). Several studies have highlighted the involvement of chronic inflammation in the development and progression of PD (Land, 2015). In rat models of PD, elevated levels of activated microglia were associated with nigrostriatal dopaminergic degeneration (Singh et al., 2011). Reducing microglia activation/reactivity could therefore be a therapeutic aim that might slow down disease progression.

A_{2A} receptors are expressed on microglia, and these receptors have been shown to play a role in regulating microglial activation. For instance, A_{2A}R deletion prevented enhanced astrogliosis and NF-κB activation caused by α-synuclein in a mouse model of PD and A_{2A}R antagonists were able to control neuroinflammation (via p38), synaptopathy and β-amyloid processing in AD models (Canas et al., 2009). Inhibition of A_{2A} receptors on microglia has been shown to lead to a reduction in the release of pro-inflammatory cytokines and an increase in the release of anti-inflammatory cytokines. This suggests that A_{2A} receptor signaling may play a role in modulating the inflammatory response of microglia, which is thought to be involved in the pathogenesis of many neurodegenerative disorders. The precise mechanisms of the A_{2A}-microglia interaction and its implications in neurodegenerative diseases are not yet fully understood. Molecular imaging techniques could help to elucidate the role of A_{2A} receptors in the brain and be applied to investigate the effects of A_{2A}-targeting interventions at a molecular level. Positron emission tomography (PET) is such a non-invasive imaging technique, which could enable the assessment of specific biological processes in the brain, such as neuroinflammation and the expression of specific receptors, as well as treatment induced changes thereon. The technique can be applied both in animals and humans and is therefore an attractive tool for translational research.

The objective of this study was to use PET imaging to evaluate the effects of 20 days of treatment with the A_{2A}R antagonist KW6002 on neuroinflammation, and D₂R availability in a unilateral intra-striatal 6-hydroxydopamine (6-OHDA) lesion model of PD in rats. Specifically, we used the tracers [¹¹C]PBR28 for neuroinflammation and [¹¹C]raclopride for D₂R availability. In addition to striatum, which plays an important role in the impaired motor function in PD, we focused on nucleus accumbens (NAc) and substantia nigra pars compacta (SNC) in the analysis of the PET images. The NAc, a key component of the brain's reward circuitry, has been implicated in the neuropsychiatric symptoms often accompanying PD (Carriere et al., 2014). The SNC, on the other hand, is the principal site of dopaminergic neuron loss in PD and plays a critical role in motor control (Chan et al., 2010; Ni and Ernst, 2022). By selecting these regions we aimed to provide a more comprehensive understanding of the effects of KW6002 on both motor and non-motor symptoms. Postmortem analysis of the brains was performed to support the imaging findings. To verify the animal model and the effect of the intervention, motor disability was assessed using the rotarod and cylinder tests.

2. Materials and methods

2.1. Experimental animals

All experiments were approved by the Dutch National Committee on Animal Experiments (CCD license: AVD1050020173069) and the Institutional Animal Care and Use Committee of the University of Groningen (IvD study number: 173069-01-004).

Outbred male Wistar rats (8–10 weeks old, n = 32, 300–400 g) were purchased from Envigo, The Netherlands. The rats were housed in groups of two in humidity (60%) and temperature controlled (21 ± 2 °C) rooms under a 12 h light–12 h dark cycle. Rats had *ad libitum* access to standard laboratory chow and water. They were allowed to acclimatize for at least 7 days after their arrival from the supplier. All experiments were performed during the light phase.

2.2. Experimental design

An overview of the study is displayed in Fig. 1. Rats were randomly divided into four groups ($n = 8$ per group). The cylinder test was performed 5 days prior to 6-OHDA injection and the rotarod test was performed 4 days prior to 6-OHDA injection to determine the baseline values in all groups. Subsequently, all rats were submitted to stereotactic injection of 6-OHDA in the right striatum. Two days after the 6-OHDA injection, groups 1 and 3 were intraperitoneally injected with vehicle solution (5% dimethyl sulfoxide, 31% polyethylene glycol 400 in saline) and groups 2 and 4 received KW6002 (3 mg/kg) dissolved in the vehicle solution. Treatment was repeated daily for the remaining 20 days. On day 3 post-surgery all groups were subjected to the rotarod test and on day 4 to the cylinder test. Groups 1 and 2 were terminated on day 7 post-surgery (peak of neuroinflammation; unpublished data) for immunoblotting analysis. On day 19 the rats from groups 3 and 4 were subjected to the cylinder test and on day 20 to the rotarod test. Dynamic $[^{11}\text{C}]$ PBR28-PET scans were performed on days 7 and 21 and $[^{11}\text{C}]$ raclopride-PET scans on day 8 and day 22 post-surgery. After the final PET scan, the rats were euthanized for immunoblotting analysis. In our study, we excluded certain animals from data quantification due to various reasons. Specifically, one animal each from vehicle treatment groups 1 and 3 were excluded because of improper transfer of neurotoxin during surgery. Additionally, we encountered a production failure of the $[^{11}\text{C}]$ PBR28 tracer on both day 7 and 21, which led to the exclusion of 1 rat from the vehicle and KW6002 treatment groups respectively. Moreover, due to $[^{11}\text{C}]$ raclopride tracer production failure on day 8, we had to exclude 1 rat each per group.

2.3. Striatal 6-OHDA lesion

Rats were anesthetized using isoflurane (5% induction, 1.5%–2.0% maintenance) and placed in a stereotactic frame with the incisor bar positioned at 0 for all injections. Body temperature was maintained by placement of the rats on a heating pad. Eye dehydration was prevented by applying eye salve. Marcaine (0.5%) was locally applied before making surgical incisions. Buprenorphine (0.01 mg/kg) was administered subcutaneously as a systemic pain medication. A longitudinal

incision along the medial line of the skull was made and the skin and fascia were pushed aside in order to expose the skull. A hole was drilled in the skull and unilateral stereotactic injections of 6-OHDA (Sigma-Aldrich) were made into the right striatum using a Hamilton syringe. A concentration of 8 μg of 6-OHDA in 0.3% ascorbic acid in saline was injected into two striatal sites (0.5 μL /site, total dose 16 μg). The following coordinates were used: (1) AP: +1.12, L: 2.6, V: 5 mm; (2) AP: +0.2, L: 3.0, V: 4.5 mm relative to bregma and ventral to the dura mater. Rate of injection was 0.5 $\mu\text{L}/\text{min}$. The syringe was left in position for 5 min at the end of injection to prevent reflux and to allow for toxin diffusion. The scalp wound was sutured and the rats were allowed to recover for 2 days before experimentation.

2.4. Behavioral testing

Motor function was assessed with the rotarod and the cylinder test. Experimental procedures are described in the supplementary material.

2.5. $[^{11}\text{C}]$ PBR28 and $[^{11}\text{C}]$ raclopride PET imaging

PET scans were acquired using a Focus 220 MicroPET camera (Siemens Medical Solutions, USA). In each scan session, one rat from the vehicle and one from the intervention group (KW6002) were scanned simultaneously. The rats were anesthetized with a mixture of isoflurane in oxygen (5% induction and 1–2% maintenance) and positioned in the camera in axial position with their heads in the field of view. A cannula was placed in a tail vein for radiotracer injection using a computer-controlled pump. The tracer solution volumes were approximately 1 mL and were injected over a period of 1 min $[^{11}\text{C}]$ PBR28 (35.6 ± 4.6 MBq; injected mass 1.43 ± 0.30 nmol) was used as a tracer for PET imaging of TSPO protein, and $[^{11}\text{C}]$ raclopride (38.6 ± 3.2 MBq; injected mass 1.05 ± 0.63 nmol) for assessing D₂R availability. The PET scans were made on two consecutive days as depicted in Fig. 1. $[^{11}\text{C}]$ PBR28 and $[^{11}\text{C}]$ raclopride were synthesized as described previously (Wang et al., 2009; Farde, 2014). A 10 min transmission scan was made to correct for scatter and attenuation of the gamma radiation by the tissue. Next, a 60 min dynamic PET scan was performed, starting at the onset of tracer injection. During the scan, the body temperature of the rats was

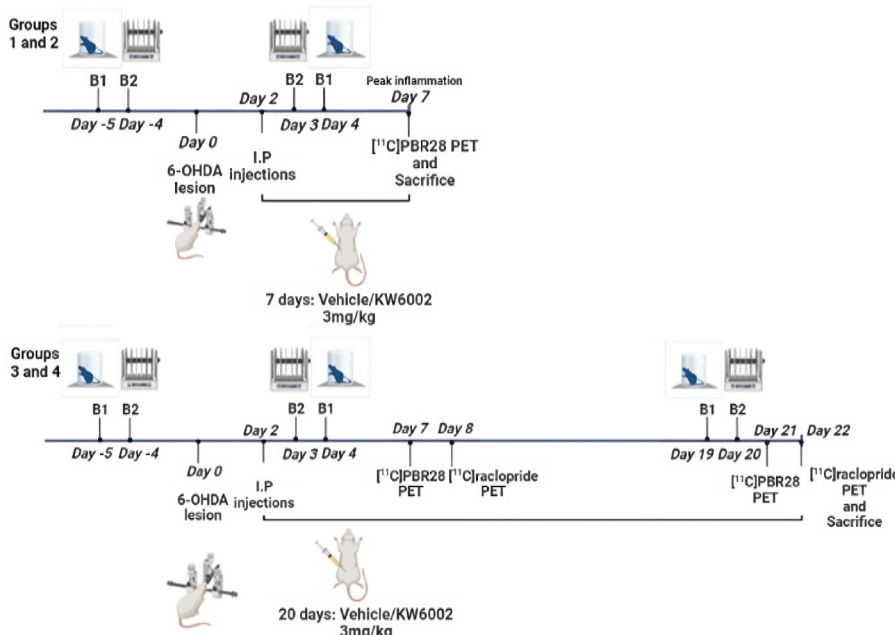


Fig. 1. Study design. Timeline of experimental procedures. Groups 1 and 2 ($n = 8$ each) were treated with either vehicle or KW6002 3 mg/kg for 7 days. Groups 3 and 4 ($n = 8$ each) were treated with either vehicle or KW6002 3 mg/kg for 20 days. B1: Cylinder test, B2: Rotarod test.

maintained using a heating pad and electronic temperature controller. The heart rate and oxygenation level of the blood of each animal were monitored with pulse oximeters. Eye dehydration was prevented by application of eye salve. After the PET scans, the rats either recovered in their home cage or were terminated for histology.

2.6. Image reconstruction and data analysis

The 60 min emission scans were divided in the following 21 frames: $6 \times 10\text{s}$, $4 \times 30\text{s}$, $2 \times 60\text{s}$, $1 \times 120\text{s}$, $1 \times 180\text{s}$, $4 \times 300\text{s}$ and $3 \times 600\text{s}$. The scans were iteratively reconstructed using an attenuation-weighted two-dimensional ordered-subset expectation maximization algorithm (4 iterations and 16 subsets) and corrected for random coincidences, scatter, radioactive decay and attenuation. The images had a slice thickness of 0.796 mm and a $256 \times 256 \times 95$ matrix with a pixel width of 0.632 mm. Using PMOD 4.1 software (PMOD Technologies LLC, Switzerland), the PET images were automatically registered to tracer-specific PET templates, that allowed the use of a predefined volume-of-interest (VOI) map of the rat brain. For [^{11}C]raclopride PET, time activity curves (TACs) were obtained for the striatum of both hemispheres and for the cerebellum. These TACs were used to calculate the non-displaceable binding potential (BP_{ND}), using the simplified reference tissue model 2 (SRTM2), with a fixed k_2 (cerebellum as reference). For [^{11}C]raclopride PET, we focused on three critical brain regions implicated in Parkinson's disease: the striatum, NAc and SNC. For [^{11}C]PBR28 PET analysis, tracer uptake in VOIs for the left and right striatum, NAc and SNC was expressed as standardized uptake value (SUV). SUV was calculated as follows: [tissue activity concentration (MBq/ml) \times body weight (g)]/[injected dose (MBq)]. The average SUV values of the last 30 min of the dynamic [^{11}C]PBR28-PET scans were used. In all animals, the ipsilateral/contralateral ratio (SUV ratio) was determined to compensate for potential differences in tracer delivery between animals.

2.7. Immunofluorescence of Iba-1

Four animals per group were anesthetized with a mixture of isoflurane in oxygen (5% induction and maintenance) and submitted to *trans*-cardiac perfusion with ice-cold 0.1 M phosphate buffered saline (PBS, pH 7.4), followed by 4% paraformaldehyde solution (PFA) dissolved in PBS. Vehicle ($n = 3$) and KW6002 ($n = 4$) brains were used for staining. These animals were selected randomly and had comparable behavioral outcome as the whole group (Supplementary Table 3). The selection of animals for staining was done randomly to minimize potential biases, and the comparable behavioral outcomes suggest that the selected animals are representative of the larger cohort. The brains were collected and post-fixed for 48 h in 4% PFA. Subsequently, the material was transferred to a solution of 30% sucrose dissolved into 0.1 M PBS. Tissues were then cut in a cryostat (Leica CM 1850) at a thickness of 7 μm . The coronal brain sections containing caudate-putamen (CPu) of the striatum and NAc were incubated overnight at 4°C with primary antibody against rabbit anti-Iba-1 (diluted 1:500, Wako), mixed with 5% of donkey serum, 1% bovine serum albumin and 0.1% Triton X-100 in PBS. Next, the brain sections were incubated with secondary antibody (Alexa Fluor 488, Invitrogen, 1:1000) for 1 h. All slides were mounted using dako mounting solution (Agilent Technologies). The material was analyzed in a Leica DM500 microscope and images of the CPu and NAc were captured. Nuclei were visualized by staining the cells with 4',6-diamidino-2-phenylindol (DAPI) dye. Using a 20x magnification, a numerical aperture of 0.5, and 488 channels, images of the CPu were acquired using tile scan in the LAS X software. Individual images were captured and were stitched into a larger image. Three brain sections per rat were analyzed using ImageJ software (NIH, USA). The number of DAPI $^+$ /Iba-1 $^+$ cells was quantified over an area that covered 1 mm^2 in the images taken from both the right and left CPu and NAc in a single animal. The absolute number of cells per mm^2 surface area was

calculated for each region (unit: cells/ mm^2). The researcher performing the stereological counting was blind to the experimental condition of the animals.

2.8. Western blotting of tyrosine hydroxylase

Four rats per group were anesthetized with a mixture of isopentane and oxygen (5% induction, 1.5%–2.0% maintenance) and submitted to *trans*-cardiac perfusion with ice-cold PBS solution. Vehicle ($n = 4$) and KW6002 ($n = 4$) brains used for staining and these animals were selected randomly had comparable behavioral outcome as the whole group (Supplementary Table 3). Striatal tissues were dissected and stored at –80 °C. These striatal tissues were homogenized for protein extraction using radioimmunoprecipitation assay (RIPA) buffer (1 M Tris HCl pH 7.6, 2 M NaCl, 10% NP-40, sodium deoxycholate, 20% sodium dodecyl sulphate (SDS)) with a protease phosphatase inhibitor. Lysates were maintained on ice for 30 min and were then sonicated and centrifuged at 10,000 rpm for 20 min at 4 °C. The supernatants were used as total protein extracts. The protein concentrations were measured using a bicinchoninic acid (BCA) protein assay. Equal amounts of total protein extracts were resolved by electrophoresis on 10% polyacrylamide gels with SDS in a running buffer. Resolved proteins were then transferred onto nitrocellulose membranes and blocked with a 10% milk solution in PBS with Tween® detergent (PBS-T). The membranes were incubated overnight with primary antibody against tyrosine hydroxylase (TH) (1:500 cat. no.ab112; Abcam) at 4 °C. After washing with PBS-T, membranes were incubated with secondary goat anti-rabbit IgG antibody conjugated with horseradish peroxidase (1:1000 IgG NA934V; GE healthcare) for 2 h at room temperature. The intensity of TH protein bands was measured by densitometry using ImageLab software (Biorad, USA). GAPDH was used as loading control. Relative density of TH for all groups was calculated by dividing individual densities of the protein in their respective lanes to the average density of the particular group. This was repeated for GAPDH. The resulting values were then used to calculate the relative optical density, which represents the ratio of the relative density of TH bands to the relative density of GAPDH bands, for all 4 experimental groups.

2.9. Statistical analysis

All statistical analyses were performed with SPSS software and Python 3.9. A generalized estimated equation model (GEE), which accounts for possible missing data, was used to analyze longitudinal data from the cylinder test, rotarod test, and PET scans. Factors used for analysis were "Time" and "Treatment". Statistical differences between two groups were assessed with the two-tailed unpaired *t*-test for DAPI $^+$ /Iba-1 $^+$ microglia quantification and relative TH intensity for individual time-points. Comparison between hemispheres was performed with a paired *t*-test for DAPI $^+$ /Iba-1 $^+$ microglia quantification. Data are expressed as mean \pm standard deviation (SD). Differences were considered statistically significant when the probability (p) value was ≤ 0.05 . Furthermore, effect sizes were estimated for PET analysis, using the Cohen's *d* index estimated from mean (M) and standard deviation (SD) according to the formula:

$$\text{Cohen's } d = (M_2 - M_1) / SD_{\text{pooled}}$$

$$SD_{\text{pooled}} = \sqrt{(SD_1^2 + SD_2^2) / 2}$$

The effect was classified as: $d > 0.2$ = small, $d > 0.5$ = medium and $d > 0.8$ = large.

3. Results

3.1. PET imaging

3.1.1. Chronic treatment with KW6002 reduces [¹¹C]PBR28 uptake in ipsilateral striatum and SNc

In this study, we tested the impact of KW6002 (3 mg/kg intraperitoneally, once daily for 20 days) on neuroinflammation using PET imaging of TSPO density, a common method for measuring neuroinflammation due to its upregulation in activated microglia (Gerhard et al., 2006). The TACs of the striatum binding of [¹¹C]PBR28-PET are shown in Supplementary Fig. 2. Fig. 2 shows representative [¹¹C]PBR28 PET images. The SUV in both striata and the ipsilateral (right)/contralateral (left) uptake ratio (I/C ratio) in striatum are presented in Table 1. There was a significant treatment effect found among the groups ($W = 21.21$, $df = 3$, $p < 0.001$). Between-group analysis showed that the I/C ratio was significantly higher for the vehicle treated compared to the KW6002 treated group on day 7 (Cohen's $d = 1.85$, $p < 0.001$) and on day 21 (Cohen's $d = 1.05$, $p = 0.045$). Longitudinal analysis performed within each group showed a time effect ($W = 18.96$, $df = 1$, $p < 0.001$). A decrease in I/C ratio was observed in the vehicle (Cohen's $d = 0.62$, $p < 0.001$) and KW6002 group (Cohen's $d = 0.85$, $p = 0.017$) between days 7 and 21 (Supplementary Fig. 3). In addition to evaluating the effects of KW6002 treatment on neuroinflammation in the striatum, its impact was also assessed in the NAc. However, there were no significant differences in the I/C ratio between groups or between timepoints (Table 1). We also investigated the effects of KW6002 treatment on neuroinflammation (activated microglia) in the SNc. The SUV and I/C ratio in the SNc are presented in Table 1. A significant treatment effect on the I/C ratio was found ($W = 15.49$, $df = 3$, $p < 0.001$). Between-group analysis revealed that the I/C ratio was significantly higher in the vehicle-treated group than in the KW6002-treated group on day 7 (Cohen's $d = 1.08$, $p = 0.038$) and on day 21 (Cohen's $d = 1.82$, $p < 0.001$). Longitudinal analysis within each group showed a significant decrease in the I/C ratio in the KW6002-treated group between days 7 and 21 (Cohen's $d = 0.75$, $p = 0.018$). No significant changes were observed in the vehicle group over time (Cohen's $d = 0.27$, $p = 0.49$).

3.1.2. [¹¹C]raclopride binding decreases after chronic administration of KW6002

The BP_{ND} of [¹¹C]raclopride was used as a marker for D_{2R} availability in the brain (Fig. 3). The TACs of the striatum binding of [¹¹C]raclopride-PET are shown in Supplementary Fig. 4. Fig. 3 shows representative [¹¹C]raclopride PET images acquired on day 8 and day 22 post-surgery, showing the striatum in each hemisphere. Statistical analysis revealed a significant main effect of treatment ($W = 17.81$, $df = 1$, $p < 0.001$) and regions ($W = 43.88$, $df = 1$, $p < 0.001$). More specifically, analysis showed that D_{2R} availability in left and right striatum was higher in vehicle treated animals than in KW6002 treated animals ($p <$

Table 1

[¹¹C]PBR28-PET SUV values in ipsilateral (right) and contralateral (left) striatum and right-to-left ratios of striatum, NAc and SNc are provided for the vehicle and KW6002 treated group for day 7 and day 21 post 6-OHDA injection. Data are reported as mean \pm SD. Significance is reported for between-group comparisons: * $p < 0.05$, ** $p < 0.01$; and for within-group comparisons: # $p < 0.05$, ## $p < 0.01$.

Region	Day 7		Day 21		
	Vehicle (n = 6)	KW6002 (n = 7)	Vehicle (n = 6)	KW6002 (n = 7)	
Striatum	Left	0.34 \pm 0.05	0.36 \pm 0.06	0.36 \pm 0.05	0.42 \pm 0.03*
	Right	0.54 \pm 0.16	0.46 \pm 0.08	0.49 \pm 0.09	0.51 \pm 0.04
	Right/ left	1.60 \pm 0.26	1.25 \pm 0.06***	1.35 \pm 0.20##	1.19 \pm 0.08**#
	Left	0.39 \pm 0.05	0.43 \pm 0.07*	0.47 \pm 0.21	0.44 \pm 0.06
	Right	0.46 \pm 0.07	0.46 \pm 0.06	0.53 \pm 0.25	0.51 \pm 0.08
	Right/ left	0.86 \pm 0.13	0.92 \pm 0.07	0.91 \pm 0.09	0.81 \pm 0.01
Nucleus accumbens	Left	0.37 \pm 0.07	0.41 \pm 0.06	0.53 \pm 0.30	0.48 \pm 0.03
	Right	0.46 \pm 0.10	0.43 \pm 0.06	0.62 \pm 0.30	0.47 \pm 0.06
	Right/ left	1.24 \pm 0.26	1.04 \pm 0.11*	1.19 \pm 0.13	0.95 \pm 0.11**

0.001). Within-group analysis showed a significantly lower D_{2R} availability in the right striatum compared to left striatum for both vehicle and KW6002 treated animals ($p < 0.001$).

On day 8, between-group analysis showed that the BP_{ND} values of both the left and right striatum of the KW6002 treated group were significantly lower than those of the vehicle group (left: Cohen's $d = 1.33$, $p = 0.03$, right: Cohen's $d = 1.40$, $p = 0.049$) (Table 2, Supplementary Fig. 5). On day 22, between-group analysis showed that the BP_{ND} values of both left and right striatum were still significantly different between the vehicle and KW6002 treated group (left: Cohen's $d = 1.01$, $p < 0.001$, right: Cohen's $d = 1.16$, $p < 0.001$).

In addition to the striatum, D_{2R} availability in the NAc was assessed. On Day 8, KW6002-treated animals showed lower D_{2R} availability in both left (Cohen's $d = 0.53$, $p = 0.08$) and right (Cohen's $d = 0.67$, $p = 0.08$) NAc compared to vehicle-treated animals, although these differences were not statistically significant (Table 2). On day 22, however, KW6002-treated animals did have significantly lower D_{2R} availability compared to the vehicle group in both left and right NAc (left: Cohen's $d = 0.92$, $p = 0.02$; right: Cohen's $d = 1.42$, $p < 0.001$) (Table 2).

We also investigated the effects of KW6002 treatment on D_{2R} availability within the SNc. Our findings indicate that KW6002 administration led to a notable decrease in D_{2R} availability in the SNc. Specifically, on day 8, the KW6002 group exhibited reduced D_{2R} availability in both the left (Cohen's $d = 0.87$, $p = 0.09$) and right SNc

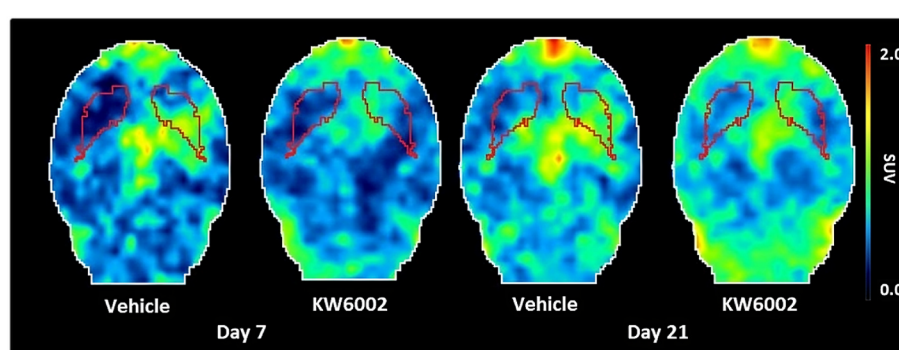


Fig. 2. [¹¹C]PBR28 uptake in the brain. (A) Representation of [¹¹C]PBR28 uptake (SUV images).

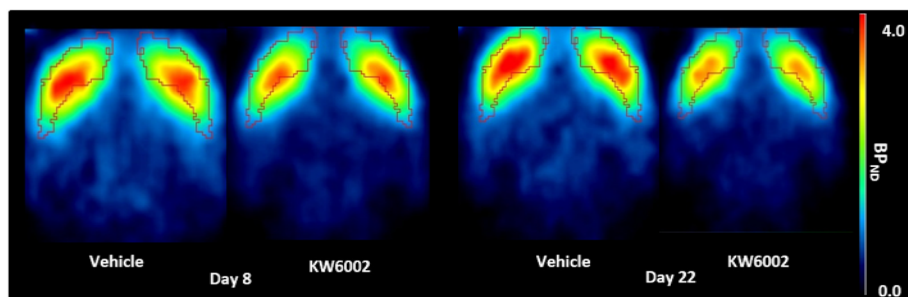


Fig. 3. $[^{11}\text{C}]$ raclopride binding in the brain. (A) Representation of $[^{11}\text{C}]$ raclopride binding (BP_{ND} images), as a surrogate marker of D_2/D_3 receptor availability in the striatum on days 8 and 22.

Table 2

$[^{11}\text{C}]$ raclopride-PET results for striatum, nucleus accumbens and substantia nigra pars compacta. BP_{ND} values are provided for the vehicle and KW6002 treated group on day 8 and day 22 post-6-OHDA injection. Data are reported as mean \pm SD. Significance is reported for between-group comparisons: * $p < 0.05$, ** $p < 0.01$; and for within-group comparisons: # $p < 0.05$, ## $p < 0.01$.

Region	Day 8		Day 22		
	Vehicle (n = 6)	KW6002 (n = 7)	Vehicle (n = 6)	KW6002 (n = 7)	
Striatum	Left	1.80 \pm 0.17	1.56 \pm 0.19*	1.83 \pm 0.28	1.56 \pm 0.25*
	Right	1.73 \pm 0.12	1.50 \pm 0.20*	1.72 \pm 0.24	1.43 \pm 0.26**#
	Left	1.05 \pm 0.16	0.97 \pm 0.04	1.20 \pm 0.09##	1.00 \pm 0.25*
	Right	1.09 \pm 0.15	0.99 \pm 0.06	1.17 \pm 0.10	0.92 \pm 0.18*
Nucleus accumbens	Left	0.41 \pm 0.08	0.35 \pm 0.03	0.38 \pm 0.10	0.27 \pm 0.08*
	Right	0.42 \pm 0.10	0.32 \pm 0.05*	0.39 \pm 0.08	0.28 \pm 0.10**

(Cohen's $d = 1.14$, $p = 0.01$) compared to the vehicle group, although this difference was only statistically significant for the ipsilateral SNc (Table 2). This pattern was sustained on day 22, where the KW6002 group continued to show significantly diminished D_2R availability in both left (Cohen's $d = 1.16$, $p = 0.01$) and right SNc (Cohen's $d = 1.20$, $p = 0.007$) relative to the vehicle-treated animals (Table 2).

3.2. Treatment with KW6002 reduced microglial reactivity in the 6-OHDA-induced lesion

Seven and 22 days after intrastriatal 6-OHDA injection, the extent of neuroinflammation was measured by stereological quantification of Iba-1 $^{+}$ cells in the striatum (Fig. 4). Injection of 6-OHDA caused a significant increase in Iba-1 $^{+}$ cells in right CPu compared to left CPu on day 7 after surgery (Vehicle: Cohen's $d = 2.6$, $t(2) = 16.73$, $p = 0.0036$; KW6002: Cohen's $d = 1.74$, $t(3) = 15.43$, $p < 0.001$) and on day 22 for vehicle (Cohen's $d = 1.35$, $t(2) = 6.12$, $p = 0.02$). There was no significant difference in Iba-1 $^{+}$ cells in right CPu compared to left CPu on day 22 after surgery for KW6002 (Cohen's $d = 1.84$, $t(3) = 3.10$, $p = 0.053$) (Table 3, Supplementary Fig. 6A). Supplementary Table 4 provides individual values for each experiment of Iba-1 immunostaining.

On day 7, the number of Iba-1 $^{+}$ cells in the right caudate-putamen was significantly higher (Cohen's $d = 1.56$, $t(5) = 5.49$, $p = 0.002$) in the vehicle group than in the KW6002 treated group. Similarly, a significantly higher (Cohen's $d = 1.28$, $t(5) = 2.643$, $p = 0.048$) number of Iba-1 $^{+}$ cells was observed in the right caudate-putamen in the vehicle group compared to the KW6002 treated group on day 22. Surprisingly, a significant reduction was also observed in left caudate-putamen in the KW6002-treated group on day 7 (Cohen's $d = 1.02$, $t(5) = 3.043$, $p = 0.028$) when compared to vehicle controls, but not on day 22 (Cohen's d

= 0.67, $t(5) = 1.036$, $p = 0.34$). In addition to caudate-putamen, Iba-1 $^{+}$ staining were quantified in NAc. On day 7 post-treatment with KW6002, there was a notable decline in Iba-1 $^{+}$ cell numbers in both left and right NAc when compared to the vehicle treated group, but this reduction was only statistically significant the right NAc (left: Cohen's $d = 1.40$, $p = 0.17$; right: Cohen's $d = 3.11$, $p = 0.009$). In contrast, on day 22, the Iba-1 $^{+}$ cell numbers in the left and right NAc did not show any significant changes (Cohen's $d = 0.38$, $p = 0.57$; Cohen's $d = 0.55$, $p = 0.50$) as detailed in Table 3 and Supplementary Fig. 6B.

3.3. Treatment with KW6002 increased tyrosine hydroxylase level in the lesioned striatum

Rat striatal tissues were processed to quantify TH protein level via western blotting analysis on days 7 and 22 to study the effect of chronic administration of KW6002 on the abundance of TH, which is an enzymatic marker for dopaminergic production (Fig. 5, Supplementary Fig. 7). On day 7 post-6-OHDA injection, no significant differences in TH level between groups were observed in either striatum (left striatum: Cohen's $d = 0.9$, $t(6) = 1.17$, p -value = 0.29, right striatum: Cohen's $d = 0.62$, $t(6) = 0.87$, p -value = 0.41; Table 4, Supplementary Fig. 8). On day 22 post 6-OHDA injection, the TH content in the left striatum of KW6002 treated rats remained the same as that of vehicle treated rats (Cohen's $d = 0.7$, $t(6) = 0.23$, $p = 0.82$). Treatment with KW6002 significantly counteracted the 6-OHDA-induced decrease in TH levels in the right striatum, compared to the rats treated with the vehicle (Cohen's $d = 0.99$, $t(6) = 3.26$, $p = 0.017$). Supplementary Table 5 provides individual values for each experiment of Western blot analysis.

3.4. KW6002 improves motor performance of rats

The impact of KW6002 on motor performance in rats with unilateral 6-OHDA lesions was assessed using the rotarod and cylinder test. KW6002 significantly improved motor function in the rotarod test, particularly the latency to fall, distance traveled, and maximum acceleration. Asymmetric forelimb use was also positively influenced by KW6002, with notable improvements in the cylinder test on day 4. A more detailed description of the results and the statistical analyses can be found in the supplementary material (Supplementary Fig. 1; Supplementary Tables 1 and 2).

4. Discussion

In our study, we observed a temporal sequence of events following 6-OHDA administration, similar to the findings of previous studies that have analyzed the time course of microglial and behavioral alterations post-6-OHDA injection (Blandini et al., 2007; Silva et al., 2016a, b; Fan and De Lannoy, 2014). The microglial activation was followed by a decrease in D_2 receptor availability and TH density in KW6002 treated animals, culminating in observable behavioral changes. KW6002

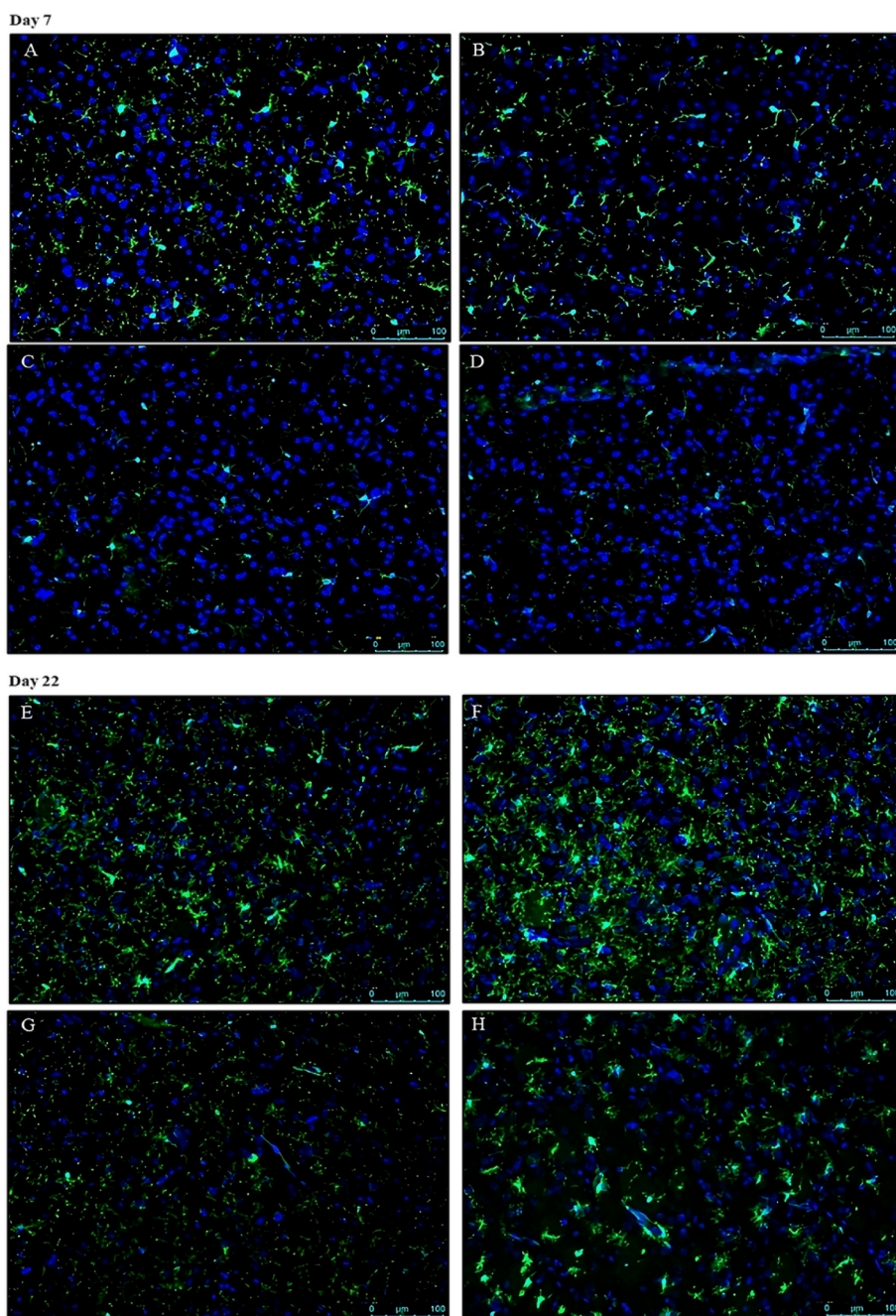


Fig. 4. Representative images from Iba1 staining of microglia in the (A) left and (B) right caudate-putamen of vehicle ($n = 3$) and in the (C) left and (D) right caudate-putamen KW6002 ($n = 4$) on Day 7. And, in the (E) left and (F) right caudate-putamen of vehicle ($n = 4$) and in the (G) left and (H) right caudate-putamen KW6002 ($n = 4$) on Day 22.

treatment appeared to reduce microglial reactivity, which was subsequently associated with a preservation of D₂ receptor availability and TH levels (Marchetti et al., 2022). This temporal mapping suggests that microglial activation may be an upstream event that triggers downstream changes in D₂ receptor and TH levels, ultimately influencing behavior. These imaging and postmortem findings were accompanied by a marked improvement in motor function in KW6002-treated animals.

4.1. KW6002 treatment improved motor performance

Unilateral 6-OHDA injection produces deficits in balance, motor coordination and rotarod performance as reported by several studies (Lundblad et al., 2003a; Monville et al., 2006; Smith et al., 2014). In

agreement with previous reports, our results show a decrease in motor function and coordination in animals after 6-OHDA lesioning. Administration of KW6002 improved the rats performance on the rotarod and in the cylinder test, which indicates that KW6002 reduced the 6-OHDA induced motor disabilities. The dose of KW6002 that we tested (3 mg/kg, daily) was based on previous rodent studies (Singh et al., 2011; Farde, 2014). Our results are in line with a previous report that showed that KW6002 treatment alone or in addition to L-DOPA, improved the rotarod performance of 6-OHDA lesioned rats (Lundblad et al., 2003b). These beneficial effects on behavior are likely due to the dampening of A_{2A} receptor activation by endogenous adenosine (Lambertucci et al., 2022). KW6002 targets the A_{2A} receptors found on the axonal terminals of both the striatal and pallidal sides of the medium spiny neurons of the

Table 3

Iba-1 immunostaining absolute cell numbers (cells/mm²) in caudate-putamen and nucleus accumbens of activated microglia 7 days and 22 days after surgery. Data is shown as mean ± SD. Statistically significant between-group differences are shown as *p < 0.05, **p < 0.01; within-group differences compared to left caudate-putamen for respective time-points are shown as #p < 0.05, ##p < 0.01, ###p < 0.001.

	Day 7		Day 22	
	Vehicle (n = 3)	KW6002 (n = 4)	Vehicle (n = 3)	KW6002 (n = 4)
Left CPu	68.2 ± 4.3	50.8 ± 9.0*	61.6 ± 16.7	50.7 ± 11.4
Right CPu	109.1 ± 30.3##	69.6 ± 10.8***##	109.8 ± 15.5#	69.8 ± 22.2*
Left NAc	77.5 ± 19.2	54.7 ± 15.2	68.1 ± 12.2	63.4 ± 12.2
Right NAc	88.2 ± 8.6	53.3 ± 13.3**	74.0 ± 13.2	64.7 ± 20.1

dopaminergic indirect pathway, which releases the indirect pathway from the excitatory effects of adenosine. This enhances the impact of dopaminergic D₂R stimulation, which leads to a reduction in the striatal indirect pathway's outflow and improves motor function (Fan and De Lannoy, 2014). Reduction of the inhibitory effect of A_{2A}Rs on the dopamine system can lead to increased dopamine neurotransmission in the basal ganglia, which can improve motor function in conditions such as Parkinson's disease, a disorder characterized by a loss of dopamine neurons in the basal ganglia (Fan and De Lannoy, 2014).

4.2. KW6002 suppresses PD associated microglial activation

Previous research has demonstrated that unilateral striatal injection of 6-OHDA results in an increased expression of microglial lysosomal enzyme marker and high accumulation of reactive microglia (Marchetti et al., 2022; Lundblad et al., 2003a; Monville et al., 2006). In the current study, we also observed an increase in the number of microglia in the 6-OHDA-treated striatum, using PET imaging - confirmed by Iba-1 staining - in the control group both on day 8 and 21. Activation of microglia after 6-OHDA administration by a toxin like 6-OHDA is known to precede the production of nitric oxide (NO) and to correlate with the expression of several pro-inflammatory markers (Pais et al., 2008). Neurotransmitter receptors on microglia can modulate cytokine synthesis and release, control iNOS expression, NO production, and the formation of free radicals that are neurotoxic (Colella et al., 2018). Dopaminergic neurons, particularly those in substantia nigra, are vulnerable to these free radicals that contribute to oxidative stress. These processes lead to increases in the extracellular levels of adenosine, which also contribute to the stimulation of microglial proliferation via A₁ and A_{2A} receptors under pathological conditions such as PD (Gomes

et al., 2013). Suppression of adenosine signaling may thus inhibit microglial activation. Moreover, the blockade of A_{2A}R has been shown to prevent the release of brain-derived neurotrophic factor (BDNF), thereby inhibiting microglial proliferation (Gomes et al., 2013). This aligns with our observation that KW6002 treatment led to a significant reduction in activated microglia. In this study, we found with [¹¹C] PBR28 PET that treatment with KW6002 mono-therapy was able to decrease the number of reactivate microglia on day 7 and 21. These results were confirmed by postmortem analysis, showing a reduction in the number of Iba-1⁺ microglial cells. By Day 21, we observed a sustained increase in microglial activation in the untreated group, whereas KW6002-treated rats showed a significant reduction in activated microglia. Our results are in line with data obtained from 1-methyl-4-phenyl-1,2,3,6-tetrahydropyridine (MPTP)-treated macaques and MPTP-lesioned marmosets, which demonstrated a neuroprotective role of A_{2A} antagonists (Ko, 2016; Uchida et al., 2015). In both days, fewer Iba-1⁺ cells were observed in the contralateral region. A likely explanation for the decrease in Iba-1 staining in the non-affected hemisphere following KW6002 treatment could be that the lesion initiates a broad activation of the brain's native immune system, especially microglia. Given its anti-inflammatory characteristics, KW6002 may successfully mitigate this activation. The importance of suppressing the microglial activation to slow down the PD disease progression has been demonstrated previously. Reducing the number of activated microglia increased the survival of dopaminergic neurons (Smith et al., 2014). KW6002 might therefore be a suitable therapeutic agent for suppressing the enhanced inflammatory response impelled by microglial cells in PD.

Administration of the neurotoxin 6-OHDA into the striatum induces retrograde degeneration of dopaminergic neurons in SNc. In this study, we found that treatment with KW6002 mono-therapy was able to decrease the uptake of the PET tracer [¹¹C]PBR28 (expressed as I/C ratio) not only in striatum, but also in the ipsilateral SNc. The decrease in tracer uptake in the SNc under KW6002 treatment is indicative of a reduced inflammatory response to 6-OHDA administration in striatum,

Table 4

Western blot densitometry data of TH level in relation to GAPDH in left and right striatum for the vehicle and KW6002 treated group for day 7 and day 22 post 6-OHDA injection. Data are reported as mean ± SD. Significance is reported as between-group: *p < 0.05.

	Day 7		Day 22	
	Vehicle (n = 4)	KW6002 (n = 4)	Vehicle (n = 4)	KW6002 (n = 4)
Left CPu	1.06 ± 0.12	0.96 ± 0.08	1.01 ± 0.12	0.99 ± 0.007
Right CPu	0.96 ± 0.20	1.05 ± 0.04	0.96 ± 0.08	1.10 ± 0.05*

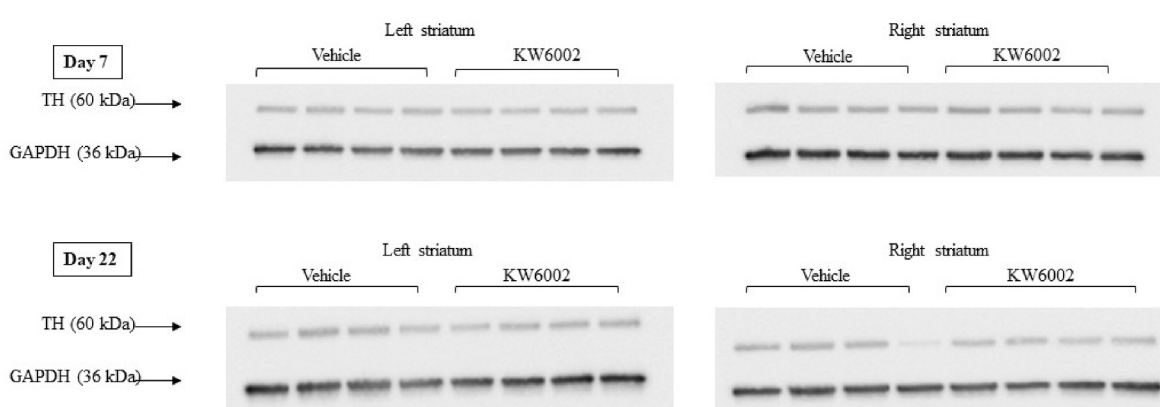


Fig. 5. Densitometry quantification of Western blot analysis for striatum level of TH subunits. Representative Western blot analysis showing protein level for TH and GAPDH subunits.

2A receptor antagonists can modulate neuroinflammation. The results align with previous studies that have investigated the role of activated microglia in the substantia nigra under pro-inflammatory conditions that mimic Parkinson's disease (Gyoneva et al., 2014; Long-Smith et al., 2009). Using lipopolysaccharide (LPS) or MPTP to induce neuroinflammation, activated microglia in the SNc were found to have reduced capacity to extend processes to damaged tissue sites. Antagonism of adenosine A_{2A} receptors restored this ability in an MPTP model of PD (Croisier et al., 2005). Interestingly, our [¹¹C]PBR28 PET analysis did not reveal significant effects within the NAc, whereas post-mortem Iba-1 staining did show a decrease in Iba-1⁺ cells in NAc on day 7 after KW6002 treatment. This discrepancy could potentially be due to the PET scan being unable to detect small differences in trace uptake, as a result of insufficient sensitivity. In addition, the so-called partial volume effect (PVE) may have played a role. The PVE causes activity spillover between adjacent tissues, resulting in a discrepancy between the recorded and true activity concentrations within a given tissue. The PVE is influenced by factors such as the dimensions of the target region, the spatial resolution of the PET camera and the contrast ratio between the target and its background (Soret et al., 2007). Thus, it is plausible that the KW6002-induced reduction in activated microglia in a small region like the NAc, as observed by Iba-1 staining, was not detected with [¹¹C]PBR28 PET because of insufficient sensitivity of the technique and/or the influence of the PVE. The activation of microglia and the subsequent inflammatory response within the NAc are implicated in the development of depressive-like behaviors (Furuyashiki and Kitaoka, 2019), which are also observed in PD. Emerging evidence suggests that neuroinflammation is a hallmark of PD, contributing to the degeneration of dopaminergic neurons and the disruption of neurotransmitter systems that regulate mood and affective behaviors (Pajares et al., 2020). Microglial activation within the NAc can exacerbate depressive symptoms by releasing pro-inflammatory cytokines (Wang et al., 2020). These cytokines can alter neuronal function and plasticity within the NAc, leading to the dysregulation of dopamine and other neurotransmitters crucial for mood regulation. This neuroinflammatory process within the NAc not only contributes to the pathophysiology of depression in PD but also offers a potential therapeutic target. This connection emphasizes the importance of the NAc and its dopaminergic and inflammatory responses. The reduction in Iba-1⁺ cells supports the notion that KW6002 possesses anti-inflammatory capabilities, likely mitigating microglial activation and thus contributing to a decrease in the inflammatory milieu associated with neuropsychiatric symptoms linked to Parkinson's disease.

4.3. Administration of KW6002 decreases D₂R availability in striatum, nucleus accumbens and substantia nigra

Previous studies have shown that dopamine depletion induced by 6-OHDA elicits an upregulation of the A_{2A}R gene in striata. The administration of 6-OHDA leads to oxidative stress-induced apoptosis of neurons, resulting in altered histone H3 acetylation in the striatum. This change in acetylation leads to decreased DNA methylation and an increase in the expression of the A_{2A}R, both in individuals with Parkinson's disease and in animals with 6-OHDA-induced lesions (Falconi et al., 2019). The imbalance between the direct and indirect dopaminergic pathways in the brain of Parkinson's patients is a result of dopaminergic neuron loss and thus a reduction in dopamine release. This leads to overactivity of the indirect pathway. The mechanism of action of A_{2A}R antagonists involves binding to the A_{2A}R within A_{2A}R-D₂R heteromeric complexes, increasing the affinity of the D₂R for dopamine and enhancing its coupling to the G-protein and subsequent its signaling.

In this study, we treated lesioned animals with KW6002 and observed a decrease in striatal [¹¹C]raclopride binding potential, and thus receptor availability in both 6-OHDA-treated and contralateral

striatum, NAc and SNc, indicating that this effect of KW6002 on D₂R-mediated signaling does not depend on the presence of neuronal damage. Interestingly, our data also revealed an impact of KW6002 on the D₂R availability in SNc, a region crucial for dopaminergic modulation in PD. The reduced D₂R availability in the SNc aligns with our striatal findings, suggesting a global downregulation of D₂R following KW6002 treatment. Upon intra-striatal injection, 6-OHDA is transported retrogradely to the SNc, selectively targeting and degenerating dopaminergic neurons. This model replicates key aspects of Parkinson's disease, including dopamine depletion and increased oxidative stress and neuroinflammation in the SNc. The heightened vulnerability of these neurons to oxidative stress is thought to stem from their elevated metabolic rates, which necessitate greater ATP production (Chan et al., 2010; Ni and Ernst, 2022). Furthermore, we extended our investigation to the NAc, a region implicated in the neuropsychiatric symptoms often accompanying PD (Mishra et al., 2018; Nucleus accumbens atrophy in Parkinson). While the NAc is primarily associated with reward and pleasure, its role in PD is increasingly recognized, particularly concerning dopamine's role in motivation and reward-seeking behavior (Bromberg-Martin et al., 2010). Recent research has also identified A_{2A} receptors in the lateral septum (LS) as key upstream regulators of stress-induced depressive-like behavior, modulating neuronal activity and signaling (Wang et al., 2023). The collective findings of the current study underscore the potential of adenosine A_{2A} antagonists like KW6002 in modulating not just motor, mood and memory but also neuropsychiatric symptoms in PD, thereby offering a more holistic treatment approach (Chen et al., 2023).

Altered D₂R binding potential after KW6002 treatment may indicate (i) an increase in the levels of endogenous dopamine, (ii) D₂R internalization upon chronic A_{2A} antagonist treatment, (iii) altered expression of the D₂ receptor gene (Ginovart, 2005; Huang et al., 2013; Schiffmann and Vanderhaeghen, 1993) or (iv) altered D₂R affinity for the radioligand as a result of allosteric interactions within the heteromeric A_{2A}R-D₂R complex. There is accumulating evidence pointing toward the potential regulation of dopamine release by A_{2A} receptors located pre-synaptically, although validation has been hindered by limitations in sensitivity (Jenner et al., 2021; Chen et al., 2001). Studies have documented presynaptic A_{2A} receptors in the glutaminergic nerve endings within the striatum that contribute to dopamine release triggered by glial cell line-derived neurotrophic factor (Garção et al., 2013; Gomes et al., 2009). However, establishing whether post-synaptic A_{2A} receptors exert regulatory control over dopamine release remains a challenge. In our study, however, a decrease in TH was observed only in the affected striatum and only on day 22 following KW6002 treatment. Therefore, it seems unlikely that increased levels of endogenous dopamine are responsible for the decrease in D₂R binding in both the ipsilateral and contralateral striatum. In fact, a post-synaptic effect of allosteric interactions of KW6002 with the heteromeric A_{2A}R-D₂R complex seems more plausible. Both A_{2A}R agonists (e.g. CGS21680) and antagonists (e.g. KW6002) were found to allosterically reduce the postsynaptic D₂R's affinity (Prasad et al., 2022).

5. Conclusions

In light of existing clinical data on KW6002, which is already an FDA-approved adjuvant treatment for Parkinson's disease, this PET study further elucidates its potential mechanisms of action. Our PET imaging and histology findings demonstrate that KW6002 mono-therapy attenuates microglial activation in the striatum and SNc following a 6-OHDA lesion. Furthermore, histology results show a decrease in microglial activation within NAc after chronic KW6002 treatment. Additionally, [¹¹C]raclopride PET and TH level indicate that chronic KW6002 treatment modulates dopaminergic function. While the precise mode of action remains to be fully understood, our study adds valuable insights into the drug's impact on neuroinflammation and dopamine signaling, which subsequently led to significant improvements in motor function.

Therefore, our results reinforce the therapeutic relevance of KW6002 as an adjunct to existing pharmacological interventions for PD.

CRediT authorship contribution statement

Kavya Prasad: Conceptualization, Data curation, Formal analysis, Visualization, Writing – original draft, Methodology, Writing – review & editing. **Erik F.J. de Vries:** Conceptualization, Methodology, Supervision, Writing – review & editing, Project administration, Resources. **Esther van der Meiden:** Data curation, Formal analysis, Writing – review & editing, Visualization. **Rodrigo Moraga-Amaro:** Writing – review & editing. **Daniel Aaron Vazquez-Matias:** Writing – review & editing. **Lara Barazzuol:** Writing – review & editing, Resources. **Rudi A. J.O. Dierckx:** Funding acquisition, Project administration, Resources, Supervision. **Aren van Waarde:** Conceptualization, Methodology, Project administration, Resources, Supervision, Writing – review & editing.

Declaration of competing interest

None.

Data availability

Data will be made available on request.

Acknowledgements

We thank Jurgen Sijbesma, Chantal Kwizera, Simon Blok and Maria Kominia, for their technical support.

Appendix A. Supplementary data

Supplementary data to this article can be found online at <https://doi.org/10.1016/j.neuropharm.2024.109862>.

References

- Agnati, L.F., Ferré, S., Lluis, C., Franco, R., Fuxe, K., 2003. Molecular mechanisms and therapeutic implications of intramembrane receptor/receptor interactions among heptahelical receptors with examples from the striatopallidal GABA neurons. *Pharmacol. Rev.* 55 (3), 509–550. <https://doi.org/10.1124/pr.55.3.2>.
- Aguazi, A., Barres, B.A., Bennett, M.L., 2013. Microglia: scapegoat, saboteur, or something else? *Science* 339 (6116), 156–161. <https://doi.org/10.1126/science.1227901>.
- Bennett, M.L., Viaene, A.N., 2021. What are activated and reactive glia and what is their role in neurodegeneration? *Neurobiol. Dis.* 148, 105172. <https://doi.org/10.1016/j.nbd.2020.105172>.
- Blandini, F., Levandis, G., Bazzini, E., Nappi, G., Armentero, M.T., 2007. Time-course of nigrostriatal damage, basal ganglia metabolic changes and behavioural alterations following intrastriatal injection of 6-hydroxydopamine in the rat: new clues from an old model. *Eur. J. Neurosci.* 25 (2), 397–405. <https://doi.org/10.1111/j.1460-9568.2006.05285.x>.
- Bromberg-Martin, E.S., Matsumoto, M., Hikosaka, O., 2010. Dopamine in motivational control: rewarding, aversive, and alerting. *Neuron* 68 (5), 815–834. <https://doi.org/10.1016/j.neuron.2010.11.022>.
- Calabresi, P., Castrioto, A., Di Filippo, M., Picconi, B., 2013. New experimental and clinical links between the hippocampus and the dopaminergic system in Parkinson's disease. *Lancet Neurol.* 12 (8), 811–821. [https://doi.org/10.1016/S1474-4422\(13\)70118-2](https://doi.org/10.1016/S1474-4422(13)70118-2).
- Canas, P.M., Porciúncula, L.O., Cunha, G.M.A., et al., 2009. Adenosine A2A receptor blockade prevents synaptotoxicity and memory dysfunction caused by β-amyloid peptides via p38 mitogen-activated protein kinase pathway. *J. Neurosci.* 29 (47), 14741–14751. <https://doi.org/10.1523/JNEUROSCI.3728-09.2009>.
- Carriere, N., Besson, P., Dujardin, K., et al., 2014. Apathy in Parkinson's disease is associated with nucleus accumbens atrophy: a magnetic resonance imaging shape analysis. *Mov. Disord.* 29 (7), 897–903. <https://doi.org/10.1002/mds.25904>.
- Chan, C.S., Gertler, T.S., Surmeier, D.J., 2010. A molecular basis for the increased vulnerability of substantia nigra dopamine neurons in aging and Parkinson's disease. *Mov. Disord.* 25 (Suppl. 1) <https://doi.org/10.1002/mds.22801>.
- Chen, J.F., Cunha, R.A., 2020. The belated US FDA approval of the adenosine A2A receptor antagonist istradefylline for treatment of Parkinson's disease. *Purinergic Signal.* 16 (2), 167–174. <https://doi.org/10.1007/s11302-020-09694-2>.
- Chen, J.F., Moratalla, R., Impagnatiello, F., et al., 2001. The role of the D2 dopamine receptor (D2R) in A2A adenosine receptor (A2AR)-mediated behavioral and cellular responses as revealed by A2A and D2 receptor knockout mice. *Proc. Natl. Acad. Sci. U.S.A.* 98 (4), 1970–1975. <https://doi.org/10.1073/pnas.98.4.1970>.
- Chen, J.F., Choi, D.S., Cunha, R.A., 2023. Striatopallidal adenosine A2A receptor modulation of goal-directed behavior: homeostatic control with cognitive flexibility. *Neuropharmacology* 226. <https://doi.org/10.1016/j.neuropharm.2023.109421>.
- Coletta, M., Zinni, M., Pansiot, J., et al., 2018. Modulation of microglial activation by adenosine A2a receptor in animal models of perinatal brain injury. *Front. Neurol.* 9 (SEP) <https://doi.org/10.3389/fneur.2018.00605>.
- Croisier, E., Moran, L.B., Dexter, D.T., Pearce, R.K.B., Graeber, M.B., 2005. Microglial inflammation in the parkinsonian substantia nigra: relationship to alpha-synuclein deposition. *J. Neuroinflammation* 2. <https://doi.org/10.1186/1742-2094-2-14>.
- Cunha, R.A., 2016. How does adenosine control neuronal dysfunction and neurodegeneration? *J. Neurochem.* 139 (6), 1019–1055. <https://doi.org/10.1111/jnc.13724>.
- Fahn, S., 2008. The history of dopamine and levodopa in the treatment of Parkinson's disease. *Mov. Disord.* 23 (Suppl. 3), S497–S508. <https://doi.org/10.1002/mds.22208>.
- Falconi, A., Bonito-Oliva, A., Di Bartolomeo, M., et al., 2019. On the role of adenosine A2A receptor gene transcriptional regulation in Parkinson's disease. *Front. Neurosci.* 13 (JUL) <https://doi.org/10.3389/fnins.2019.00683>.
- Fan, J., De Lannoy, I.A.M., 2014. Pharmacokinetics. *Biochem Pharmacol.* 87 (1), 93–120. <https://doi.org/10.1016/j.bcp.2013.09.007>.
- Farde, L., 2014. Quantitative analysis of D2 dopamine receptor binding in the living human brain by PET author (s): lars Farde , Håakan Hall, Erling Ehrin and Göran Sedvall 231 (4735), 258–261.
- Ferré, S., Bonaventura, J., Zhu, W., et al., 2018. Essential control of the function of the striatopallidal neuron by pre-coupled complexes of adenosine A2A-dopamine D2 receptor heterotrimers and adenylyl cyclase. *Front. Pharmacol.* 9 (APR), 1–18. <https://doi.org/10.3389/fphar.2018.00243>.
- Furyashiki, T., Kitaoka, S., 2019. Neural Mechanisms Underlying Adaptive and Maladaptive Consequences of Stress: Roles of Dopaminergic and Inflammatory Responses. <https://doi.org/10.1111/pcn.12901/full>. Published online.
- Fuxe, K., Agnati, L.F., Jacobsen, K., et al., 2003. Receptor heteromerization in adenosine A2A receptor signaling: relevance for striatal function and Parkinson's disease. *Neurology* 61 (11 Suppl. 6), S19–S23. <https://doi.org/10.1212/01.wnl.0000095206.44418.5c>.
- Galvan, A., Devengnäs, A., Wichmann, T., 2015. Alterations in neuronal activity in basal ganglia-thalamocortical circuits in the parkinsonian state. *Front. Neuroanat.* 9, 5. <https://doi.org/10.3389/fnana.2015.00005>.
- Garcão, P., Szabó, E.C., Wopereis, S., et al., 2013. Functional interaction between pre-synaptic α6β2-containing nicotinic and adenosine A2A receptors in the control of dopamine release in the rat striatum. *Br. J. Pharmacol.* 169 (7), 1600–1611. <https://doi.org/10.1111/bph.12234>.
- Gehrman, J., Matsumoto, Y., Kreutzberg, G.W., 1995. Microglia: intrinsic immunoeffector cell of the brain. *Brain Res. Rev.* 20 (3), 269–287. [https://doi.org/10.1016/0165-0173\(94\)00015-H](https://doi.org/10.1016/0165-0173(94)00015-H).
- Gerfen, C.R., Surmeier, D.J., 2011. Modulation of striatal projection systems by dopamine. *Annu. Rev. Neurosci.* 34, 441–466. <https://doi.org/10.1146/annurev-neuro-061010-113641>.
- Ginovart, N., 2005. Imaging the dopamine system with *in vivo* [11C]raclopride displacement studies: understanding the true mechanism. *Mol. Imaging Biol.* 7 (1), 45–52. <https://doi.org/10.1007/s11307-005-0932-0>.
- Gomes, C.A.R.V., Simões, P.F., Canas, P.M., et al., 2009. GDNF control of the glutamatergic cortico-striatal pathway requires tonic activation of adenosine A2A receptors. *J. Neurochem.* 108 (5), 1208–1219. <https://doi.org/10.1111/j.1471-4159.2009.05876.x>.
- Gomes, C., Ferreira, R., George, J., et al., 2013. Activation of microglial cells triggers a release of brain-derived neurotrophic factor (BDNF) inducing their proliferation in an adenosine A2A receptor-dependent manner: a2A receptor blockade prevents BDNF release and proliferation of microglia. *J. Neuroinflammation* 10, 16. <https://doi.org/10.1186/1742-2094-10-16>.
- Gyoneva, S., Shapiro, L., Lazo, C., et al., 2014. Adenosine A2A receptor antagonism reverses inflammation-induced impairment of microglial process extension in a model of Parkinson's disease. *Neurobiol. Dis.* 67, 191–202. <https://doi.org/10.1016/j.nbd.2014.03.004>.
- Hillion, J., Canals, M., Torvinen, M., et al., 2002. Coaggregation, cointernalization, and codesensitization of adenosine A2A receptors and dopamine D2 receptors. *J. Biol. Chem.* 277 (20), 18091–18097. <https://doi.org/10.1074/jbc.M10731200>.
- Huang, L., Wu, D.D., Zhang, L., Feng, L.Y., 2013. Modulation of A2a receptor antagonist on D2 receptor internalization and ERK phosphorylation. *Acta Pharmacol. Sin.* 34 (10), 1292–1300. <https://doi.org/10.1038/aps.2013.87>.
- Ikeda, K., Kurokawa, M., Aoyama, S., Kuwana, Y., 2002. Neuroprotection by adenosine A2A receptor blockade in experimental models of Parkinson's disease. *J. Neurochem.* 80 (2), 262–270. <https://doi.org/10.1046/j.0022-3042.2001.00694.x>.
- Jenner, P., Mori, A., Aradi, S.D., Hauser, R.A., 2021. Istradefylline—a first generation adenosine A2A antagonist for the treatment of Parkinson's disease. *Expert Rev. Neurother.* 21 (3), 317–333. <https://doi.org/10.1080/14737175.2021.1880896>.
- Kalia, L.V., Lang, A.E., 2015. Parkinson's disease. *Lancet (London, England)* 386 (9996), 896–912. [https://doi.org/10.1016/S0140-6736\(14\)61393-3](https://doi.org/10.1016/S0140-6736(14)61393-3).
- Ko, W.K.D., 2016. An Evaluation of Istradefylline Treatment on Parkinsonian Motor and Cognitive Deficits in July.

- Lambertucci, C., Marucci, G., Catarzi, D., et al., 2022. A(2A) adenosine receptor antagonists and their potential in neurological disorders. *Curr. Med. Chem.* 29 (28), 4780–4795. <https://doi.org/10.2174/092986732966220218094501>.
- Land, W.G., 2015. The role of damage-associated molecular patterns in human diseases: Part I - promoting inflammation and immunity. *Sultan Qaboos Univ Med J* 15 (1), e9–e21.
- Li, Q., Barres, B.A., 2018. Microglia and macrophages in brain homeostasis and disease. *Nat. Rev. Immunol.* 18 (4), 225–242. <https://doi.org/10.1038/nri.2017.125>.
- Long-Smith, C.M., Sullivan, A.M., Nolan, Y.M., 2009. The influence of microglia on the pathogenesis of Parkinson's disease. *Prog Neurobiol* 89 (3), 277–287. <https://doi.org/10.1016/j.pneurobio.2009.08.001>.
- Lundblad, M., Vaudano, E., Cencio, M.A., 2003a. Cellular and behavioural effects of the adenosine A2a receptor antagonist KW-6002 in a rat model of L-DOPA-induced dyskinesia. *J. Neurochem.* 84 (6), 1398–1410. <https://doi.org/10.1046/j.1471-4159.2003.01632.x>.
- Lundblad, M., Vaudano, E., Cencio, M.A., 2003b. Cellular and behavioural effects of the adenosine A2a receptor antagonist KW-6002 in a rat model of L-DOPA-induced dyskinesia. *J. Neurochem.* 84 (6), 1398–1410. <https://doi.org/10.1046/j.1471-4159.2003.01632.x>.
- Marchetti, B., Giachino, C., Tirolo, C., Serapide, M.F., 2022. "Reframing" dopamine signaling at the intersection of glial networks in the aged Parkinsonian brain as innate Nrf2/Wnt driver: therapeutic implications. *Aging Cell* 21 (4), 1–25. <https://doi.org/10.1111/acel.13575>.
- Mishra, A., Singh, S., Shukla, S., 2018. Physiological and functional basis of dopamine receptors and their role in neurogenesis: possible implication for Parkinson's disease. *J. Exp. Neurosci.* 12 <https://doi.org/10.1177/1179069518779829>.
- Monville, C., Torres, E.M., Dunnett, S.B., 2006. Comparison of incremental and accelerating protocols of the rotarod test for the assessment of motor deficits in the 6-OHDA model. *J. Neurosci. Methods* 158 (2), 219–223. <https://doi.org/10.1016/j.jneumeth.2006.06.001>.
- Morelli, M., Carta, A.R., Jenner, P., 2009. Adenosine A2A receptors and Parkinson's disease. *Handb. Exp. Pharmacol.* 193, 589–615. https://doi.org/10.1007/978-3-540-89615-9_18.
- Ni, A., Ernst, C., 2022. Evidence that substantia nigra pars compacta dopaminergic neurons are selectively vulnerable to oxidative stress because they are highly metabolically active. *Front. Cell. Neurosci.* 16 <https://doi.org/10.3389/fncel.2022.826193>.
- Nucleus Accumbens Atrophy in Parkinson's Disease (Mavridis' Atrophy) 10 Years Later. Obeso, J.A., Rodríguez-Oroz, M.C., Benítez-Temino, B., et al., 2008. Functional organization of the basal ganglia: therapeutic implications for Parkinson's disease. *Mov. Disord.* 23 (Suppl. 3), S548–S559. <https://doi.org/10.1002/mds.22062>.
- Pais, T.F., Figueiredo, C., Peixoto, R., Braz, M.H., Chatterjee, S., 2008. Necrotic neurons enhance microglial neurotoxicity through induction of glutaminase by a MyD88-dependent pathway. *J. Neuroinflammation* 5 (1), 43. <https://doi.org/10.1186/1742-2094-5-43>.
- Pajares, M., I Rojo, A., Manda, G., Boscá, L., Cuadrado, A., 2020. Inflammation in Parkinson's disease: mechanisms and therapeutic implications. *Cells* 9 (7). <https://doi.org/10.3390/cells9071687>.
- Prasad, K., De Vries, E.F.J., Sijbesma, J.W.A., et al., 2022. Impact of an adenosine A2AReceptor agonist and antagonist on binding of the dopamine D2Receptor ligand [¹¹C]raclopride in the rodent striatum. *Mol. Pharm.* 19 (8), 2992–3001. <https://doi.org/10.1021/acs.molpharmaceut.2c00450>.
- Ramesh, G., MacLean, A.G., Philipp, M.T., 2013. Cytokines and chemokines at the crossroads of neuroinflammation, neurodegeneration, and neuropathic pain. *Mediat. Inflamm.* 2013, 480739. <https://doi.org/10.1155/2013/480739>.
- Ray Dorsey, E., Elbaz, A., Nichols, E., et al., 2016. Global, Regional, and National Burden of Parkinson's Disease, 1990–2016: a Systematic Analysis for the Global Burden of Disease Study. *Lancet Neurol.* [https://doi.org/10.1016/S1474-4422\(18\)30295-3](https://doi.org/10.1016/S1474-4422(18)30295-3). Published online 2018.
- Richardson, P.J., Kase, H., Jenner, P.G., 1997. Adenosine A2A receptor antagonists as new agents for the treatment of Parkinson's disease. *Trends Pharmacol. Sci.* 18 (9), 338–344. [https://doi.org/10.1016/s0165-6147\(97\)01096-1](https://doi.org/10.1016/s0165-6147(97)01096-1).
- Schiffmann, S.N., Vanderhaeghen, J.J., 1993. Adenosine A2 receptors regulate the gene expression of striatopallidal and striatonigral neurons. *J. Neurosci.* 13 (3), 1080–1087. <https://doi.org/10.1523/jneurosci.13-03-01080.1993>.
- Silva, T.P da, Poli, A., Hara, D.B., Takahashi, R.N., 2016a. Time course study of microglial and behavioral alterations induced by 6-hydroxydopamine in rats. *Neurosci. Lett.* 622, 83–87. <https://doi.org/10.1016/j.neulet.2016.04.049>.
- Silva, T.P da, Poli, A., Hara, D.B., Takahashi, R.N., 2016b. Time course study of microglial and behavioral alterations induced by 6-hydroxydopamine in rats. *Neurosci. Lett.* 622, 83–87. <https://doi.org/10.1016/j.neulet.2016.04.049>.
- Singh, A.K., Tiwari, M.N., Dixit, A., et al., 2011. Nigrostriatal proteomics of cypermetrin-induced dopaminergic neurodegeneration: microglial activation-dependent and -independent regulations. *Toxicol. Sci.* 122 (2), 526–538. <https://doi.org/10.1093/toxsci/kfr115>.
- Smith, K.M., Browne, S.E., Jayaraman, S., et al., 2014. Effects of the selective adenosine A2A receptor antagonist, SCH 412348, on the parkinsonian phenotype of MitoPark mice. *Eur. J. Pharmacol.* 728 (1), 31–38. <https://doi.org/10.1016/j.ejphar.2014.01.052>.
- Soret, M., Bacharach, S.L., Buvat, I., 2007. Partial-volume effect in PET tumor imaging. *J. Nucl. Med.* 48 (6), 932–945. <https://doi.org/10.2967/jnumed.106.035774>.
- Tufekci, K.U., Meuwissen, R., Genc, S., Genc, K., 2012. Inflammation in Parkinson's disease. *Adv Protein Chem Struct Biol* 88, 69–132. <https://doi.org/10.1016/B978-0-12-398314-5.00004-0>.
- Tysnes, O.B., Storstein, A., 2017. Epidemiology of Parkinson's disease. *J. Neural. Transm.* 124 (8), 901–905. <https://doi.org/10.1007/s00702-017-1686-y>.
- Uchida, S.I., Soshiroda, K., Okita, E., et al., 2015. The adenosine A2A receptor antagonist, istradefylline enhances anti-parkinsonian activity induced by combined treatment with low doses of L-DOPA and dopamine agonists in MPTP-treated common marmosets. *Eur. J. Pharmacol.* 766, 25–30. <https://doi.org/10.1016/j.ejphar.2015.09.028>.
- Vaamonde, J., Ibáñez, R., Gudín, M., Hernández, A., 2003. [Fluctuations and dyskinésias as early L-dopa-induced motor complications in severe Parkinsonian's patients]. *Neurología* 18 (3), 162–165.
- Wang, M., Yoder, K.K., Gao, M., et al., 2009. Fully automated synthesis and initial PET evaluation of [¹¹C]PBR28. *Bioorg. Med. Chem. Lett.* 19 (19), 5636–5639. <https://doi.org/10.1016/j.bmcl.2009.08.051>.
- Wang, J., Lai, S., Li, G., et al., 2020. Microglial activation contributes to depressive-like behavior in dopamine D3 receptor knockout mice. *Brain Behav. Immun.* 83 (June 2019), 226–238. <https://doi.org/10.1016/j.bbi.2019.10.016>.
- Wang, M., Li, P., Li, Z., et al., 2023. Lateral septum adenosine A2A receptors control stress-induced depressive-like behaviors via signaling to the hypothalamus and habenula. *Nat. Commun.* 14 (1) <https://doi.org/10.1038/s41467-023-37601-x>.
- Zhai, S., Shen, W., Graves, S.M., Surmeier, D.J., 2019. Dopaminergic modulation of striatal function and Parkinson's disease. *J. Neural. Transm.* 126 (4), 411–422. <https://doi.org/10.1007/s00702-019-01997-y>.